Oxygen isotope/salinity relationship in the northern Indian Ocean

Gilles Delaygue, Edouard Bard, Claire Rollion, Jean Jouzel, Michel Stiévenard, Jean-Claude Duplessy, Gerald Ganssen

JOURNAL OF GEOPHYSICAL RESEARCH, VOL. 106, NO. C3, PAGES 4565–4574, MARCH 15, 2001

Oxygen isotope/salinity relationship in the northern Indian Ocean

Gilles Delaygue,[1,2] Edouard Bard, and Claire Rollion

Centre Européen de Recherche et d'Enseignement des Géosciences de l'Environnement, Aix-en-Provence, France

Jean Jouzel, Michel Stiévenard, and Jean-Claude Duplessy

Laboratoire des Sciences du Climat et de l'Environnement, CEA Saclay, Gif-sur-Yvette, France

Gerald Ganssen

Department of Earth Sciences, Free University Amsterdam, Amsterdam, Netherlands

Abstract. We analyze the surface $\delta^{18}O$ - salinity relationships of the Bay of Bengal and the Arabian Sea, in the northern Indian Ocean, known for their contrasting hydrological conditions. New measurements of these tracers show a very low $\delta^{18}O$ - salinity slope associated with the strong dilution in the Bay of Bengal, but a slope more typical of this latitude in the Arabian Sea. Although this region is marked by a complex monsoonal regime, numerical modeling using a box model and a general circulation model is able to capture the $\delta^{18}O$ - salinity slope and its geographical variation. Both models clearly show that the low $\delta^{18}O$ - salinity slope is due to the evaporation-minus-precipitation balance, with an important contribution of the continental runoff in the Bay of Bengal. Although the low value of these slopes (~0.25) makes past salinity reconstructions uncertain, insight into the Last Glacial Maximum conditions shows a probable stability of these slopes and limited error on paleosalinity.

1. Introduction

Hydrological studies of the northern Indian Ocean have focused on the flux divergence of vapor in order to refine both the mechanism and the vapor source of the monsoon precipitation over India. *Cadet and Reverdin* [1981] estimated the Arabian Sea contribution to the monsoonal precipitation to be about 20%, the remainder originating from the Southern Hemisphere. They showed a large increase in the evaporation-minus-precipitation (*E-P*) balance over the Arabian Sea at the onset of the monsoon, with no counterpart in the Bay of Bengal. This *E-P* budget is very different between the basins even on an annual basis [*Trenberth and Guillemot*, 1998]. Continental runoff is another contributor to the oceanic surface hydrology not accounted for in these atmospheric studies. Because of the geography of the continental drainage area, the monsoonal precipitation does not runoff into the Arabian Sea but, instead, flows to the Bay of Bengal. Hence the river discharges into both basins are different by an order of magnitude. As a consequence of these geographical differences, a dilution of the surface waters is obvious in the Bay of Bengal where the typical salinity is about 2 less than south of India (Figure 1). Still, it is difficult to separate the respective effects of precipitation and runoff to this dilution.

Among the hydrological characteristics of the oceanic waters the ^{18}O content (the $H_2{}^{18}O/H_2{}^{16}O$ ratio R, hereafter expressed as the deviation δ with respect to the Vienna standard mean ocean water (VSMOW) value, in permil: $\delta^{18}O = (R/R_{SMOW} - 1)1000$) is rarely used because of the measurement difficulties. Together with the salinity and other tracers, it can serve to characterize a water mass [e.g., *Craig and Gordon*, 1965; *Pierre et al.*, 1994] and to disentangle the different contributions to a water mixture [e.g., *Östlund and Hut*, 1984]. The $\delta^{18}O$ and salinity variations covary in the oceanic surface because they both arise from a balance among (1) an enrichment due to evaporation, (2) a depletion due to precipitation and runoff, and (3) a mixing due to oceanic advection and diffusion. Their spatial relationship is linear, and it is characteristic of different basins and latitudes [*Craig and Gordon*, 1965]. Craig and Gordon were able to reproduce this relationship with a simple box model but only on the global scale, mainly because of the lack of observations. With the increasing atmospheric and oceanic data it is now possible to test their model on a more local scale in order to clarify the $\delta^{18}O$ - salinity relationship. The case of the tropical Indian Ocean is made complex by the strong role of the evaporation in the hydrological budget, unlike in high latitudes, and by the monsoonal perturbation.

This $\delta^{18}O$ - salinity relationship is also important in the field of paleoclimatology. The $\delta^{18}O$ measurements from carbonate sediments have been used to estimate sea surface salinity variations, which are basic for the understanding of past oceanic dynamics [e.g., *Broecker*, 1990; *Duplessy et al.*, 1991] and past monsoon intensity [*Duplessy*, 1982; *Rostek et al.*, 1993]. Such a salinity reconstruction is based on the slope of the $\delta^{18}O$ - salinity temporal relationship, i.e., the ratio of the past-to-present variations Δ ($\Delta\delta^{18}O/\Delta S$). Instead, the observed spatial slope is used, i.e., the

[1]Also at Laboratoire des Sciences du Climat et de l'Environnement, Commissariat à l'Energie Atomique de Saclay, Gif-sur-Yvette, France.

[2]Now at Department of Geophysical Sciences, University of Chicago, Chicago, Illinois.

Paper number 1999JC000061.
0148-0227/01/1999JC000061$09.00

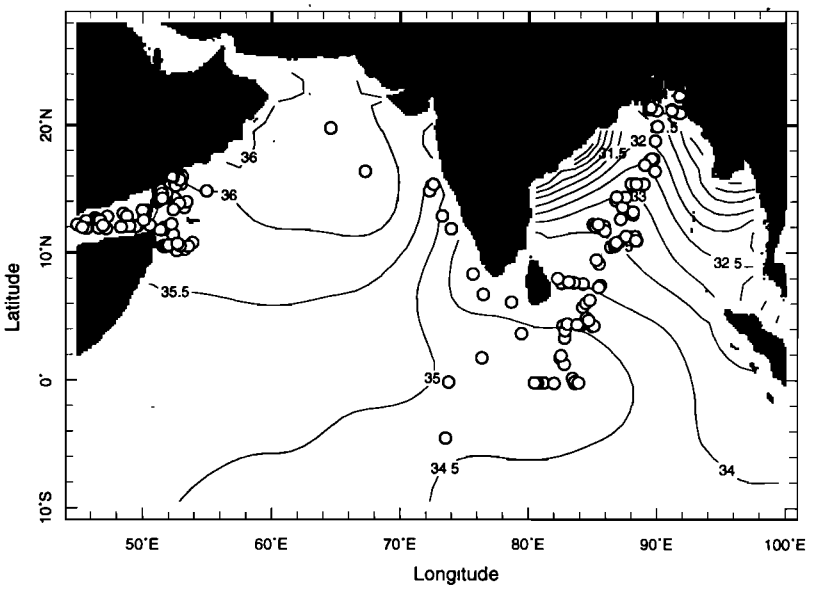

Figure 1. Hydrological contrast between the Arabian Sea (western basin) and the Bay of Bengal (eastern basin) expressed by the annual salinity [*Levitus et al.*, 1994]. Circles correspond to the locations of the water samples used for $\delta^{18}O$ - salinity correlation.

$\Delta\delta^{18}O/\Delta S$ ratio, where Δ is the spatial variation. *Rohling and Bigg* [1998] pointed out the possibility of an important change of this spatial relationship in the past and thus of the inadequacy of this method. *Schmidt* [1999] estimated that half of the uncertainty in reconstructing past salinity arose from the difference between spatial and temporal slopes. Using an ocean general circulation model, he also showed [*Schmidt*, 1998] that temporal and spatial gradients may not be equal over timescales of season to decades.

By comparing new observations and modeling results we aim to improve the understanding of the $\delta^{18}O$ - salinity relationship in a complex tropical region, the northern Indian Ocean, where it is of importance for paleoreconstruction. Besides the simple model of *Craig and Gordon* [1965], we test the ability of a general circulation model implemented with the isotope, which succeeds in simulating the $\delta^{18}O$ - salinity relationship on the global scale [*Delaygue et al.*, 2000]. First, we summarize the atmospheric budget of the Arabian Sea and the Bay of Bengal; then we present new surface $\delta^{18}O$ and salinity measurements; and finally, we discuss them with the help of modeling.

2. Atmospheric Forcings of the Northern Indian Ocean

The atmospheric budget on both oceanic sides of India is quite contrasted. Over the Arabian Sea the annual net divergence flux (E-P) is strongly positive (about 1 m yr^{-1} or 3 mm d^{-1}), as opposed to a negative divergence flux (about -0.4 m yr^{-1} or -1 mm d^{-1}) over the Bay of Bengal [*Trenberth and Guillemot*, 1998]. On the seasonal scale the difference is even more pronounced, with a divergence peaking locally to 20 mm d^{-1} over the Arabian Sea during summer (June-August, JJA) [*Peixóto and Oort*, 1983]. This contrast is mostly due to the monsoonal summer precipitation, which falls on the Bay of Bengal but not on the Arabian Sea, except along the southwest Indian coast. An indicative limit of about 0.7 m yr^{-1} (2 mm d^{-1}) for the annual precipitation can be used to separate both basins [*Trenberth and Guillemot*, 1998]. During the summer monsoonal period (JJA) an enormous quantity of moisture is transported over the Arabian Sea to the Indian continent (0.4 Sv, 1 Sv $\equiv 10^6$ m^3 s^{-1}) [*Hastenrath and Greischar*, 1993], part of which flows to the Bay of Bengal. On the other hand, the evaporation is less different between the basins: it increases similarly during the summer because of oceanic heat release and during the winter because of continental winds due to the reversed continent-ocean temperature gradient (the "dry" monsoon). An annual evaporation flux of 1.3 m yr^{-1} (3.5 mm d^{-1}) has been estimated for the northern Indian Ocean by *Hastenrath and Greischar* [1993].

The continental runoff strongly contributes to the hydrology contrast in the northern Indian Ocean. The main rivers flowing into the Bay of Bengal, the Ganges, Brahmaputra, and Irrawaddy, originate in the area receiving the monsoonal precipitation and total 1500 km^3 yr^{-1} (0.05 Sv) [*Perry et al.*, 1996]. Spread over the whole Bay of Bengal (about 2x 10^6 km^2), this flux represents about 2 mm d^{-1}, the same magnitude as precipitation. The respective dilution effects of the runoff and precipitation fluxes thus depend on their mixing through the Bay of Bengal. In contrast, the main discharge into the Arabian Sea, the Indus, flows north of the Himalayan barrier and brings only about 190 km^3 yr^{-1} (0.006 Sv).

These geographical characteristics strongly contribute to differentiate the surface waters in both basins (Figure 1), with low salinities in the Bay of Bengal (typically lower than 34) and high salinities in the Arabian Sea (typically higher than 36). A meridional gradient also exists throughout the year, opposite in both basins: the southern part is less saline than the northern one in the Arabian Sea and, conversely, in the Bay of Bengal [*Levitus et al.*, 1994]. These reversed meridional gradients are maintained by the opposite forcing over each basin (the evaporation surplus over the Arabian Sea and the dilution by runoff and precipitation excess over the Bay of Bengal) and the oceanic exchanges between the basins.

The seasonal variability of salinity is also different in the basins. In the Arabian Sea the strongest variation of about 2 takes

place in the southern part (9°N) and along the Indian coast (strongly diluted by the summer precipitation), but it is less than 0.5 north of 15°N. In the Bay of Bengal a variation of 10 happens in the northern part (18°N), reduced to 1 at 12°N. These contrasts between the basins also hold for the $\delta^{18}O$ and its relationship with salinity.

3. The $\delta^{18}O$ Measurements and Relation to Salinity

A new set of 78 water measurements from the Bay of Bengal, obtained from samples collected during the 1993-1994 campaign of the German R/V *Sonne* ("SO93"), is presented here. The collection occured during January-February 1994, i.e., during the winter monsoon with low precipitation and runoff. Sample locations are shown in Figure 1. These surface water samples were taken underway, between the hydrological stations, and sealed in glass bottles. The $\delta^{18}O$ was measured at the Laboratoire des Sciences du Climat et de l'Environnement (LSCE) with a Finnigan MAT 252, by CO_2 equilibration. At least two measurements were performed for each sample. The overall (analytical and reproducibility) standard error on $\delta^{18}O$ is about 0.05‰. Because of a technical problem with the embarked salinograph, salinity was not measured onboard, but instead, it was determined at the laboratory (Centre Océanologique de Marseille, France) by conductimetry using the same water samples as for the $\delta^{18}O$ measurements (and after these measurements). Because of the limited water volume left, salinity measurements were performed in triplicate only for 8 samples, in duplicate for 35 samples, and once for 6 samples. No measurements were possible for the 29 other samples. Their salinity was, instead, interpolated between the two closest hydrological stations of the campaign for which precise measurements exist [*Quadfasel et al.*, 1994]. To estimate the accuracy of this interpolation procedure, we compare the measured and interpolated salinities for the other samples of the southern area. The standard deviation of these differences is 0.3, for the whole Bay of Bengal. Actually, these 29 samples all originate from the southern part of the Bay of Bengal, where the spatial gradient of salinity is weak compared to the northern part. This prevents the formation of a strong bias due to this interpolation. We thus use the interpolated salinities to one decimal point.

For the Arabian Sea, new measurements from the Netherland Institute for Sea Research (NIOZ) program (Dutch R/V *Tyro* campaigns 1992-1993) are combined with a set of 16 measurements published by *Östlund et al.* [1987] and *Duplessy et al.* [1981]. The Netherland Indian Ocean Program (NIOP) was devoted to the study of the monsoon effects on the marine ecosystem, especially in the Gulf of Aden and along the coast of Somalia. The different campaigns happened during the winter and summer monsoons (Table 1). Surface water was sampled at the hydrological stations. Salinity and $\delta^{18}O$ were measured at the Free University, Amsterdam. The $\delta^{18}O$ was measured by CO_2 equilibration with a Finningan MAT 251 mass spectrometer. The precisions on salinity and $\delta^{18}O$ measurements are 0.1 and 0.1‰, respectively.

Table 1. The Different Sets of Subsurface $\delta^{18}O$ and Salinity Measurements Used in This Study

Campaign	Date	Number of data
	Bay of Bengal	
SO-93	Jan.-Feb. 1994	78
	Arabian Sea	
GEOSECS station 416 [*Östlund et al.*, 1987]	Dec. 1977	7
Osiris II-MD10 [*Duplessy et al.*, 1981]	June-July 1976	13
NIOP B0-C0	May-June 1992	6
NIOP B2	Jan.-Feb. 1993	11
NIOP C1	Aug.-Sept. 1992	36
NIOP C2	Feb.-March 1993	39

In the Bay of Bengal, salinity and $\delta^{18}O$ display a northward decrease. From the equator to about 15°N, most points range between 35 and 33 for salinity and 0 and 0.5‰ for $\delta^{18}O$. Northward, salinity and $\delta^{18}O$ decrease down to 23 and -2‰, respectively. Still, an approximate linear relationship is observed with a correlation coefficient of $r = 0.97$, namely, $\delta^{18}O = 0.18S - 5.9$ (Figure 2). All linear regressions discussed in this paper are tabulated in Table 2 with the standard deviations associated to each regression parameter. Sampling was done during January and February, i.e., during the winter monsoon with low precipitation and runoff.

In the Arabian Sea, typical enriched values are found with salinity up to 36.6 and $\delta^{18}O$ up to 0.9‰. Both salinity and $\delta^{18}O$ display a very limited range of values, about 1.5 for salinity and 0.5‰ for $\delta^{18}O$. We do not use here all of the available data for two reasons: (1) during the summer monsoon the strong upwelling occuring along the Somalia coast brings deep waters to the surface, with specific characteristics, and for this reason the Somalian part of the NIOP expeditions (Table 1) are not used; (2) some bias may occur between different sets of measurements. With this perspective the NIOP set, measured in the same laboratory, is fully consistent. An earlier set of nine samples from the Osiris IV-MD19 campaign (July-August 1979), measured at LSCE, shows a similar slope but with a systematic shift and has not been used. Though a weaker correlation ($r = 0.80$), which may be partly explained by their limited range, $\delta^{18}O$ and salinity display a linear relationship: $\delta^{18}O = 0.27S - 9.2$. We note that spanning mainly the Gulf of Aden, these data represent a very limited, also very specific area, compared to the whole Arabian Sea. Still, these waters interest us in two ways. Their $\delta^{18}O$ - salinity relationship may not be so different from the rest of the Arabian basin, given their latitude. In this case the rest of the Arabian Sea would have the same linear relationship. Alternatively, these waters may contribute to the Arabian Sea surface by mixing. In this case they would constitute an end-member in the $\delta^{18}O$ - salinity diagram, but the actual relationship for the whole Arabian Sea may have a different slope.

The seasonal variability of $\delta^{18}O$ and its relationship with salinity are difficult to address with the available data. For the Gulf of Aden the different NIOP campaigns have been conducted in the same area under extreme seasons (Table 1). Thus the derived relationship already accounts for the seasonal variability. The weak $\delta^{18}O$ - salinity slope (0.27) implies a limited variation of $\delta^{18}O$ over the year since the salinity variation is <0.5 [*Levitus et al.*, 1994]. For the Somali Basin, $\delta^{18}O$ varies roughly between 0.4 and 0.6‰ and does not show any clear correlation with salinity. This could be related, during the summer monsoon, to the upwelling of deep waters. The composition of the deep waters is very homogeneous and thus displays a weak correlation between $\delta^{18}O$ and salinity. Alternatively, this correlation may be due to the atmospheric forcing since such a weak correlation is characteristic

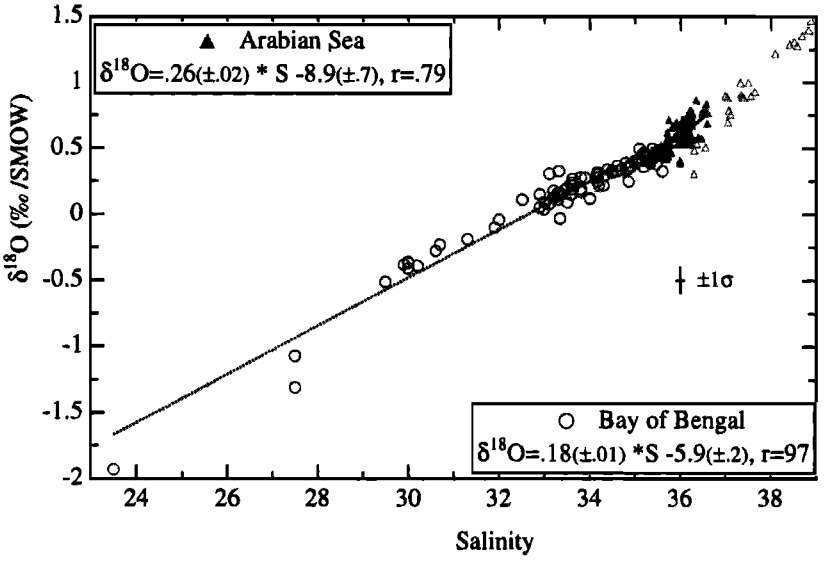

Figure 2. Surface $\delta^{18}O$ - salinity relationships for the northern Indian Ocean based on the data sets of Table 1. The Arabian Sea (solid triangles) is mainly represented by the Gulf of Aden and displays a strong salinity and $\delta^{18}O$ enrichment partly due to mixing with the Red Sea (open triangles) [*Ganssen and Kroon*, 1991]. The Bay of Bengal (open circles) is characterized by a strong dilution. The linear regressions (Table 2) of these relationships are also shown, with obvious differences in the slope and correlation. Error bars represent the maximum $\pm\sigma$ uncertainties on the measurements. Locations of the samples are shown on Figure 1.

of the tropical surface waters [*Craig and Gordon*, 1965]. For the Bay of Bengal, sample collection was restricted to 2 months. Thus it is not possible to discuss the seasonal variability of the $\delta^{18}O$ – salinity relationship, especially considering the pronounced salinity variation. For both regions, modeling an annual relationship close to the observed one (next paragraph) gives some confidence in its seasonal stability despite the $\delta^{18}O$ and salinity variations.

4. Modeling the $\delta^{18}O$ - Salinity Relationship

These measurements of $\delta^{18}O$ and salinity show that besides their contrasting distributions, they also display contrasting relationships between the northern Indian basins. If the stronger precipitation(+runoff)-to-evaporation ratio in the Bay of Bengal readily explains its dilution compared to the Arabian Sea, two components still remain unclear. First, the respective roles of the precipitation and runoff to this dilution are not well known. Second, from subtropics to high latitudes a similar increase of the precipitation-to-evaporation ratio increases this slope, contrary to what is observed here between the two basins. Modeling this slope can help to separate the different effects and determine their variations in the past. We use both a multibox model and a general circulation model to test the effect of the atmospheric forcing on the $\delta^{18}O$ and salinity distribution and relationship. This atmospheric forcing comprises water (E, P, and R for the runoff) and isotopic fluxes ($E\delta e$, $P\delta p$ and $R\delta r$, where δe, δp and δr are the isotopic contents of the evaporation, precipitation, and runoff). Our modeling is original in that these fluxes are consistently derived from an atmospheric model and the simulation has reached a pseudo-equilibrium. More details concerning this modeling are given by *Delaygue et al.* [2000].

These fluxes are derived from the NASA/Goddard Institute for Space Studies (GISS) atmospheric general circulation model (GCM) [*Hansen et al.*, 1983]. This model features representations of the major hydrological processes affecting the oxygen isotopes of the water and calculates isotopic fluxes between the ocean and atmosphere for each grid point [*Jouzel et al.*, 1987]. The simulated isotopic content of precipitation compares reasonably well with observations on the global scale. For the evaporation the lack of isotopic measurements prevents any comparison. Over the Indian Ocean the simulated isotopic content δp can be compared with the Global Network for Isotopes in Precipitation (GNIP) measurements, an International Atomic Energy Agency (IAEA)/World Meteorological Organization program (The GNIP Database, IAEA/WMO, Vienna, Austria, 1998, available at http://www.iaea.org/programs/ri/gnip/gnipmain.htm). Though mainly restricted to the continents, these data have been "objectively" interpolated on the global scale by R. Mathieu et al. (Isotopes in precipitation: A global view, manuscript in preparation, 2000). Precipitation over the Bay of Bengal shows an annual $\delta^{18}O$ value around -4.5‰, with a small seasonal range (± 1‰) and is slightly enriched over the Arabian Sea (-3.5‰ annually, ± 1‰). The GISS model predicts precipitation as slightly too depleted over the Bay of Bengal (between -4.5 and -5.5‰), and slightly too enriched over the Arabian Sea (between -2.5 and -3.5‰).

River runoff is estimated by combining the GISS GCM precipitation to the drainage scheme of *Miller et al.* [1994]. We only calculate an annual average, equally dispatched over the 12 months, that totals 2300 $km^3\ yr^{-1}$ in the Bay of Bengal and 290 $km^3\ yr^{-1}$ in the Arabian Sea. This is 50% more than the estimations of *Perry et al.* [1996], but they may underestimate the actual flux in the Bay of Bengal (R. Murtugudde, NASA Goddard Space Flight Center, Greenbelt, Maryland, personal communication, 2000). Few measurements of the runoff isotopic composition are available. In the Bay of Bengal the Ganges-Brahmaputra complex shows a seasonal variation between -6‰ in winter and -10‰ after the monsoon season, with an annual weighted average around -9±1‰ [*Ramesh and Sarin*, 1992; C. France-Lanord, Centre de Recherches Pétrologiques et Géochimiques, France, personal communication, 1997]. This depletion associated with the

Table 2. Linear Regressions of the $\delta^{18}O$ - Salinity Spatial Relationships From Measurements and Simulations Detailed in This Study [a]

	Number of Data	Slope (±σ)	Intercept (±σ)	Correlation Coefficient *r*
		Bay of Bengal		
Measurements (SO 93 campaign)	78	0.18 (±0.01)	-5.9 (±0.2)	0.97
OPA model	96	0.22 (±0.01)	-7.3 (±0.2)	0.97
OPA model (north of 8°N)	96	0.19 (±0.01)	-6.4 (±0.3)	0.97
OPA model without runoff	96	0.40 (±0.004)	-13.6 (±0.2)	0.99
Box model (open ocean points)	87	0.36 (±0.01)	-12.4 (±0.4)	0.96
(points with runoff)	9	0.14 (±0.01)	-4.7 (±0.2)	0.99
Box model without runoff	96	0.35 (±0.01)	-12.0 (±0.4)	0.95
Box model without runoff for LGM	96	0.33 (±0.01)	-10.4 (±0.5)	0.94
		Arabian Sea		
Measurements	112	0.26 (±0.02)	-8.9 (±0.6)	0.79
OPA model	163	0.27 (±0.01)	-8.9 (±0.4)	0.88
OPA model without runoff	163	0.29 (±0.01)	-9.8 (±0.3)	0.93
Box model	163	0.19 (±0.01)	-6.2 (±0.2)	0.94
Box model without runoff	163	0.21 (±0.01)	-6.8 (±0.2)	0.93
Box model without runoff for LGM	163	0.27 (±0.01)	-8.2 (±0.3)	0.95

[a] The model grid points cover the northern part of the Indian Ocean from the equator, except where specified.

monsoon is due to the contribution of the Himalayan part of the drainage area, which receives depleted water moisture, as well as to the so-called "amount effect", i.e., a correlation between the precipitation amount and the isotopic depletion [*Dansgaard*, 1964]. In the Arabian Sea the only reported runoff composition is cited by *Rohling and Bigg* [1998], showing depleted values between -11.5‰ and -9‰. The isotopic runoff composition derived from the GISS fluxes is largely too enriched, about -4.5‰ in both basins.

Although these isotopic contents are different from the observed ones, they are consistent with the water fluxes simulated by the GISS GCM. Thus we can expect the net water and isotopic fluxes (equations (1) and (2)) to be closer than each individual value to the real ones. These net fluxes that represent the atmospheric forcing are applied to two different oceanic models.

4.1. Multibox Model

Craig and Gordon [1965] interpreted the $\delta^{18}O$ - salinity relationship at the ocean surface with a one-box model. The atmospheric budget in this surface box is balanced by a vertical advective/diffusive flux from a deep, homogeneous reservoir. The oceanic parameters of this model consist in the vertical advective/diffusive flux and the ^{18}O and salinity compositions of the deep reservoir. *Juillet-Leclerc et al.* [1997] inferred these oceanic parameters by correlating the $\delta^{18}O$ and salinity surface compositions from the Geochemical Ocean Sections Study (GEOSECS) [*Östlund et al.*, 1987] with the GISS GCM atmospheric fluxes. Following Juillet-Leclerc et al., we use a two-dimensional array of surface boxes spanning the northern Indian Ocean and force them with the GISS GCM fluxes. Water and salt budgets for each surface box allow estimation of the stationary salinity as

$$S = S_0 * \frac{Q}{P + R - E + Q}, \qquad (1)$$

where S_0 is the salinity of the oceanic deep reservoir (34.6‰) and Q is the vertical advection/diffusion flux derived by *Juillet-Leclerc et al.* [1997] ($Q = 4.85 \times 10^{-4}$ mm s^{-1}). This flux can be considered as a fit parameter, allowing realistic values of salinity to be modeled. Accounting for a mixed layer depth of 100 m, this value leads to a vertical diffusion coefficient of 5×10^{-5} m^2 s^{-1}, which is consistent with the usual oceanographic value. The $\delta^{18}O$ is estimated consistently as

$$\delta^{18}O = \frac{P\delta p + R\delta r - E\delta e + Q\delta_0}{P + R - E + Q}, \qquad (2)$$

where δ_0 is the isotopic composition of the deep oceanic reservoir as derived by *Juillet-Leclerc et al.* [1997] ($\delta_0 = 0.2$‰). Equation (2) is more accurate than the simplified one used by *Juillet-Leclerc et al.* [1997], because in some cases the term $P+R-E$ can be comparable to Q because of strong runoff.

For each surface box of the Indian Ocean array we apply monthly atmospheric fluxes to estimate the $\delta^{18}O$ and salinity (equations (1) and (2)) of an ideal ocean surface in equilibrium with these fluxes. For some coastal boxes we prescribe a continental runoff R. For these boxes we also compute the surface composition without this runoff ($R = 0$). For these boxes, and only for them, we thus estimate two different $\delta^{18}O$ and salinity compositions, with and without runoff. The other boxes are not affected by this runoff in any way since the box model has no lateral mixing. These estimated $\delta^{18}O$ and salinity compositions, annually averaged, are plotted in Figures 3a and 3b.

For the Arabian Sea the $\delta^{18}O$ - salinity relationship without runoff (Figure 3a) is close to the observed one to within 20% (slope and intercept). Adding a runoff flux in some points (Figure 3b) has very little effect. On the contrary, for the Bay of Bengal the predicted slope (0.35) is significantly higher than the observed one (0.18) without runoff, and the salinity minimum is not low enough (Figure 3a). However, the compositions of boxes with runoff do show a marked dilution, even stronger than in the observations, and a lower slope close to the observed one (Figure 3b and Table 2). The box model thus allows characterization of specifically the effect of the runoff since there is no exchange between the boxes.

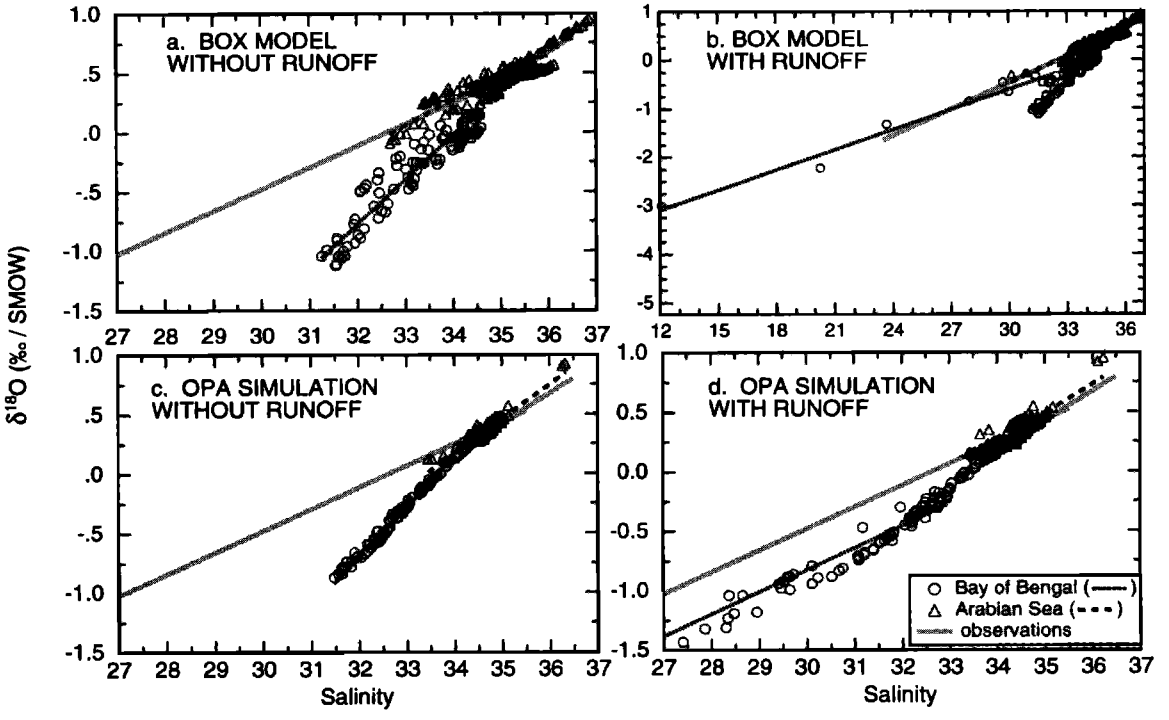

Figure 3. The $\delta^{18}O$ and salinity values simulated for the northern Indian Ocean surface by two different models forced with the same atmospheric fluxes (i.e., precipitation, continental runoff, and evaporation). (a)-(b) *Craig and Gordon*'s [1965] box model does not include any horizontal advection, which is treated by the (c)-(d) oceanic GCM OPA. Modeling allows isolation of the effect of the runoff by including it (Figures 3b and 3d) or not (Figures 3a and 3c). Linear regressions (Table 2) are also shown and compared with the observed ones. Despite the different scales used for Figure 3b, because of the strong dilution, the *y/x* ratio is the same as for the other graphs.

This model allows us to address the seasonal variability of the $\delta^{18}O$ - salinity relationship without considering the effect of the runoff. This relationship is found to be poorly defined (weak correlation) during the summer months. We average the slopes and intercepts of the $\delta^{18}O$ - salinity relationship of the months with a correlation coefficient r higher than 0.8. For the Bay of Bengal the mean slope is then 0.33 (over these months the standard deviation is ±.06) and the mean intercept is -11.3(±2.0), and for the Arabian Sea, they are 0.26(±.05) and -8.7(±1.9), respectively. Therefore, except for few months when the correlation is barely significant, the same annual $\delta^{18}O$ - salinity relationship seems to hold throughout the year.

Thus this box model reproduces the low $\delta^{18}O$ - salinity slope characteristic of the tropical zone. In the Bay of Bengal it also predicts a strong impact of the runoff on this slope, in contrast to the Arabian Sea. However, since there is no exchange between boxes, the dilution effect of the runoff is restricted to some coastal boxes. In order to extend this dilution effect to the whole basin we now apply the same atmospheric fluxes to a GCM, which provides a more realistic oceanic circulation.

4.2. General Circulation Model

We account for the oceanic circulation by implementing the $^{18}O/^{16}O$ ratio in an oceanic GCM. Briefly, we prescribe the GISS GCM isotopic fluxes to a tracer version of the Laboratoire d'Océanographie Dynamique et de Climatologie, Paris, Océan Parallélisé (OPA) oceanic GCM [*Madec et al.*, 1998]. The water $^{18}O/^{16}O$ ratio is then advected by the model as a passive tracer. The spatial resolution is about 4°x1° (longitude x latitude) in this Indian region. A fine vertical resolution (10 levels in the first 100 m) and a parameterization of the vertical diffusivity by turbulent kinetic energy scheme allow for a precise description of the atmosphere-sea exchange.

Since the OPA model salinity is calculated with an atmospheric forcing different from the GISS fluxes, this salinity is not fully consistent with the $\delta^{18}O$, and this could bias their relationship. Thus we simulate an additional passive tracer whose surface variations are forced by the *E-P* budget of the GISS fluxes. This tracer is thus comparable to salinity from its hydrological origin, but it has no feedback on the oceanic circulation. The important point here is that it is consistent with the ^{18}O tracer because (1) their variations are forced by the same GISS atmospheric fluxes and (2) they are mixed by the same model circulation. Thus, even if the absolute values of $\delta^{18}O$ and salinity are not perfectly reproduced, we expect from this consistency a better simulation of their relationship. We thus use this hydrological tracer, called "salinity" in the following for the sake of simplicity, for correlating with the $\delta^{18}O$. The simulation starts with an ocean homogeneous for both tracers and lasts 2200 years. As with the box model, we test the dilution effect of the runoff on the $\delta^{18}O$ - salinity relationship. With this aim we selectively prevent any continental discharge in the northern Indian Ocean and proceed with the simulation during 60 years.

Figure 4 presents the spatial distribution of the simulated annual $\delta^{18}O$, as well as the anomaly due to the runoff. The simulated salinity distribution displays the same pattern. Since the sparse measurements do not allow a similar reconstruction, we can compare this simulated distribution with the reconstruction of

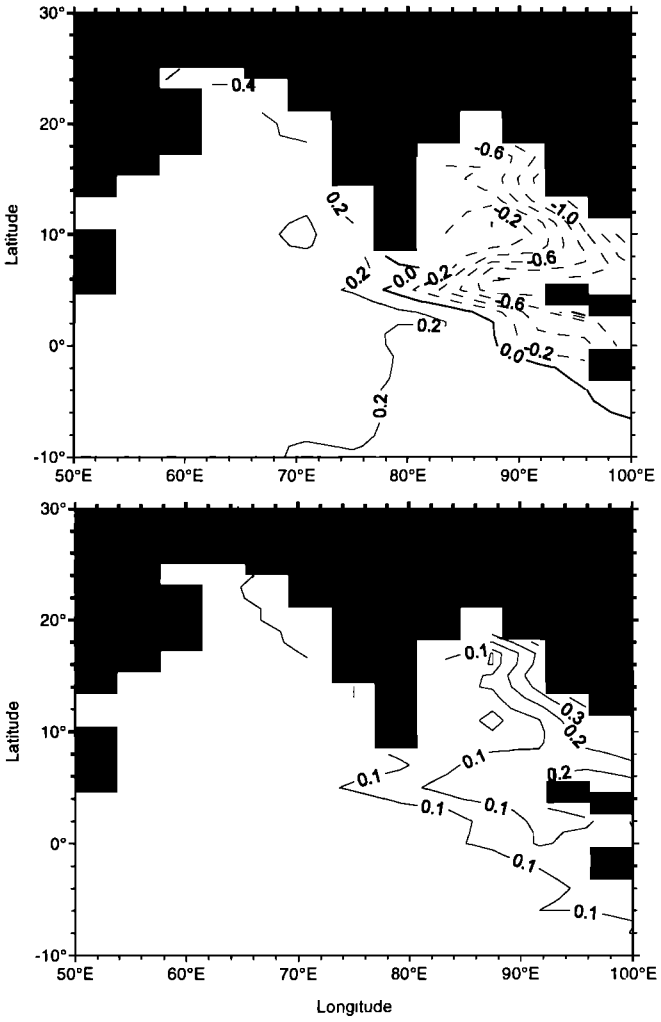

Figure 4. Distribution of annual surface $\delta^{18}O$ simulated in the northern Indian Ocean with the OPA oceanic GCM after 2200 years: (top) simulation with runoff and (bottom) difference between simulations without and with runoff. The spatial resolution of this model in this region is about 4°x1° (longitude x latitude). The $\delta^{18}O$ values are expressed in permil with respect to VSMOW.

Duplessy [1982] based on Holocene core top carbonate $\delta^{18}O$ composition. The simulated gradients correspond well in the Bay of Bengal (about 1‰ through the bay) but are too low in the Arabian Sea (0.6‰ observed but 0.4‰ in our simulation from south to north). Both distributions agree on the location of the highest $\delta^{18}O$ values, found in the Gulf of Oman (>0.6‰ in the simulation), and of the lowest, along the northeast side of the Bay of Bengal, due to both the runoff (Ganges, Brahmaputra, and Irrawadi) and the precipitation. Without runoff the $\delta^{18}O$ increases everywhere but mainly in the Bay of Bengal, by up to 0.3‰. This distribution proves the atmospheric forcing, although derived from a GCM, to be reasonable at first order.

Figures 3c and 3d present the simulated relationships of $\delta^{18}O$ and salinity without and with runoff, respectively. Compared to the box model results (Figures 3a and 3b), the scattering of the points and the range of each variable are reduced. This can be readily explained by the mixing between boxes.

Without runoff the relationships are similar to the ones found in the box model. In the Bay of Bengal the minima of both $\delta^{18}O$ and salinity are higher than in the real ocean, that is, the dilution is less marked, by 0.8‰ and 5 respectively. The $\delta^{18}O$ - salinity slope (0.40) is significantly higher than the observed one (0.18). In the Arabian Sea the observed range of $\delta^{18}O$ and salinity is well simulated as is the slope of their relationship (0.29 compared to 0.27 in the observations).

Adding runoff in the basins does not significantly change the Arabian Sea characteristics, neither for the spatial distribution nor for the relationship with a slope of 0.27 (Figure 3d). However, it greatly dilutes the Bay of Bengal, with $\delta^{18}O$ and salinity values as low as -2‰ and 22, and lowers the $\delta^{18}O$ - salinity slope to 0.22, a value closer to that observed (0.18). These slopes are not distinct within 2σ (Table 2). The simulated intercept is significantly different from the observed one (-7.3‰ and -5.9‰, respectively, with a standard deviation of 0.2). In fact, since both slopes are not equal, the $\delta^{18}O$ shift between the relationships depends on the salinity at which it is calculated, and its uncertainty is lowest close to the mean value of salinity (33.27 for observations and 31.70 for OPA simulation). For $S = 32.5$ this $\delta^{18}O$ shift is 0.26‰. It is large compared to climatic variations, for instance, but limited when compared to the error on the isotopic forcing (by 0.5‰ on the precipitation composition and 5‰ on the runoff composition; see section 4). When only the area of the Bay of Bengal northward of 8°N (tip of India) is considered, the simulated relationship ($\delta^{18}O = 0.19S - 6.4$) is even closer to the observed one. The difference lies in the boxes that connect the basins and present an $\delta^{18}O$ - salinity relationship intermediate to both basins.

These model results show, quite consistently, that in the Bay of Bengal the runoff, and not only the *E-P* budget, partly determines the $\delta^{18}O$ - salinity relationship. In the Arabian Sea the *E-P* budget is sufficient to reproduce the observations. The oceanic circulation seems important in mixing the runoff, thereby diluting the waters and slightly lowering the slope, but the atmospheric fluxes play the primary role since even a crude representation with the box model gives some reasonable result. We now try to separate the contributions of these atmospheric fluxes to the $\delta^{18}O$ - salinity relationship, especially the strong impact of the runoff. We then address the problem of using this relationship for past salinity reconstruction.

5. Discussion

5.1. The $\delta^{18}O$ - Salinity Relationship As a Mixing Line

Studies focusing on the $\delta^{18}O$ - salinity relationship have been based on two assumptions: first, that this relationship is generated by mixing oceanic and freshwater end-members and, second, that the freshwater component consists of the balance between evaporation, precipitation, and continental runoff. This latter balance has been often simplified to the sole runoff in studies of coastal and high-latitude regions, where it is actually an important term [e.g., *Fairbanks*, 1982], and because of the difficulty in addressing the evaporation flux. With this simplification, estimation of runoff isotopic content for glacial climate has been proposed in order to predict a past $\delta^{18}O$ - salinity relationship [*Rohling and Bigg*, 1998; *Schäfer-Neth*, 1998]. However, as stressed by *Craig and Gordon* [1965], the assumption considering the runoff as the main term is generally not valid for the open ocean since the runoff is negligible in the global hydrological budget.

The box model is a useful way to convert the atmospheric fluxes into oceanic variations of salinity and $\delta^{18}O$. It allows writing of the $\delta^{18}O$ - salinity relationship as such a mixing line be-

tween an oceanic end-member ($S = S_0$, $\delta = \delta_0$) and the freshwater end-member ($S = 0$, $\delta = I$):

$$\delta^{18}O = \frac{\delta_0 - I}{S_0 - 0} S + I \,. \quad (3)$$

I is the intercept in the $\delta^{18}O$ - salinity diagram, and actually depends on evaporation, precipitation, and runoff:

$$I = \frac{P\delta p + R\delta r - E\delta e}{P + R - E}. \quad (4)$$

The negative sign for E expresses the enrichment due to the evaporation. In the $\delta^{18}O$ - salinity diagram the evaporation can be thought of as an end-member weighted by $-E$ (compared to P and R). Of course, such a box model is very simplified since it lacks any oceanic horizontal advection, but comparison with observations shows that it works reasonably well. From the dependence of I (equation (4)), it becomes clearer that the intercept I is generally different from δr since in the open ocean the dilution effect from the continental runoff R is generally not significant compared to P-E (see discussion by *Craig and Gordon* [1965]). For the open ocean surface on the global scale the GEOSECS intercept I = -17.5‰ can be readily explained by equation (4) and not by the runoff, as is sometimes claimed, by using the mean values δe = -4‰ and δp = -2.5‰ (since δr is more depleted), E = 1 m yr^{-1} and P = 0.9 m yr^{-1}.

In contrast, in a coastal area where the runoff R may be important compared to P-E the intercept I is closer to δr. This extreme case has been realistically simulated in the Bay of Bengal (Figures 3b-3d). It is shown schematically in Figure 5 by using averaged values for this region derived from the GISS model. Note that $\delta^{18}O$ and salinity values higher than δ_0 and S_0 are predicted by (1) ($P+R-E<0$ leads to $S>S_0$). Without runoff (R = 0) a low intercept I (-13.4‰) defines a high $\delta^{18}O$ - salinity slope (0.39).

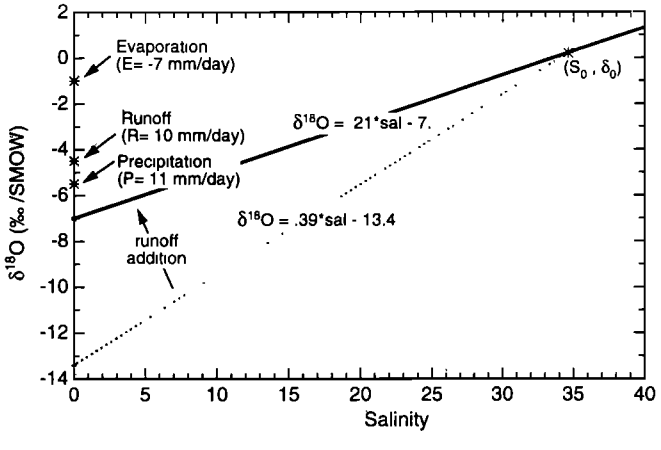

Figure 5. Schematic diagram of the present-day $\delta^{18}O$ - salinity relationship for the Bay of Bengal, assuming it is a mixing line between oceanic and freshwater end-members. The "pure" oceanic composition is taken from the study of *Juillet-Leclerc et al.* [1997]. The freshwater one is derived from the GISS GCM: mean values of precipitation and evaporation (fluxes and isotopic compositions) are estimated for the Bay of Bengal and define a strong slope (stippled line). Addition of runoff with an isotopic composition predicted from the GISS GCM lowers this slope. The value of the runoff flux, which represents the dilution of the runoff flow in the Bay of Bengal, is adjusted so as to get a realistic slope. A value close to the precipitation flux is actually required.

Adding the continental runoff R increases the intercept I and lowers the $\delta^{18}O$ - salinity slope, as simulated by both the box model and GCM (Figure 3). Quantitatively, a runoff flux approximately equivalent to the precipitation ($R \approx P$) is required in order to reproduce the observed slope and intercept. This required runoff flux (10 mm d^{-1}) represents a dilution of the total runoff (2300 km^3 yr^{-1} prescribed in the models, 0.07 Sv) spread over half the Bay of Bengal (~10^6 km^2). In the Arabian Sea, adding the runoff only slightly lowers the slope (from 0.29 to 0.27 with the GCM) because the runoff term R is not significant compared to P-E.

Figure 5 stresses the difference between the intercept I and the runoff composition δr. Both in the Bay of Bengal and in the Arabian Sea the isotopic compositions of the rivers prescribed in our simulations are significantly different from the intercepts simulated by the GCM. The prescribed river compositions are homogeneous within 0.5‰ because of the low spatial resolution of the GISS model, with a weighted average of -4.5‰. This is different from the intercepts of -7.3‰ in the Bay of Bengal and -8.9‰ in the Arabian Sea (Table 2).

As underlined in section 4, the water and isotopic fluxes derived from the GISS model and prescribed to the oceanic models are somewhat different from the real ones. However the simulation of realistic $\delta^{18}O$ values as well as the $\delta^{18}O$ - salinity relationship confirms that the consistency of these fluxes is more important than their absolute values. This first-order consistency appears good enough to drive adequately the ocean surface composition. Still, the difference between real and model fluxes introduces some bias, for instance, the shift between observed and simulated intercepts in the Bay of Bengal.

5.2. Consequence of Climatic Change

Since the multibox model is able to reproduce the basics of the modern $\delta^{18}O$ - salinity relationship, we apply the GISS model atmospheric fluxes corresponding to the Last Glacial Maximum (LGM) conditions [*Jouzel et al.*, 1994]. In both basins the simulated evaporation and precipitation fluxes decrease, especially the precipitation in the Bay of Bengal due to a drop of the monsoonal intensity. The runoff is not used here because the relationship between the flow and the actual dilution of the ocean is not trivial, as is shown in section 4.

In the Arabian Sea the LGM $\delta^{18}O$ - salinity slope is close to the modern observed one and slightly higher than the modern simulated one (Table 2). In the Bay of Bengal the slope is similar to the modern one without runoff. Thus the slope appears quite stable in both basins when the runoff is not accounted for, with a value typical of the intertropical zone.

Since the intensity of the summer monsoon has dropped, runoff could become less important for the Bay of Bengal. However, the isotopic fluxes $E\delta e$ and $P\delta p$ over this basin are very close to each other; thus the intercept I is expected (equation (4)) to be more sensitive to the runoff isotopic composition δr. This LGM runoff composition is unlikely to be very different from the modern one. Changes of the precipitation isotopic composition simulated by the GISS model [*Jouzel et al.*, 1994] over the Indian drainage basin are small and in opposite directions. A decrease of $\delta^{18}O$ over the colder Himalayan region is balanced by an increase due to the monsoon intensity drop (from the amount effect). Thus, assuming an intercept I_{LGM} close to the runoff composition, between -4 and -5‰, the slope of the $\delta^{18}O$ - salinity LGM relationship would range between 0.15 and 0.20 (accounting for the global oceanic $\delta^{18}O$ and salinity enrichments, by 1‰ [*Schrag et al.*, 1996]). This range is quite similar to modern values of the

$\delta^{18}O$ - salinity slope, observed (0.18) as well as simulated (0.15-0.21 with the box model; see Figure 5).

5.3. Spatial versus Temporal Slopes

Even if the $\delta^{18}O$ - salinity slope were stable under different climates, this would not allow us to use such a spatial slope for reconstructing paleosalinity. The temporal slope must be considered instead, i.e., the slope relating the time variations of $\delta^{18}O$ and salinity, which is very difficult to estimate. The error on using the spatial slope is reduced by accounting for the global oceanic salinity and $\delta^{18}O$ changes (about 1‰), even if they are actually not precisely known [*Schmidt*, 1999]. The salinity and $\delta^{18}O$ variations left by this global correction are due to local hydrological changes. They are assumed to be related by the modern $\delta^{18}O$ - salinity spatial slope, and this is the cause of some possible bias on the reconstructed paleosalinity. This bias can be quantified from knowing the precise value of the LGM spatial slope, denoted a' (where a is the modern one). The local variations ΔS and $\Delta\delta$ of salinity and isotope, between modern and past climates, are related by $\Delta S = \Delta\delta/a'$, but inferred as $\Delta S = \Delta\delta/a$. The error ε on the inferred ΔS thus amounts to $\varepsilon = \Delta\delta(a-a')/(aa')$. For the Bay of Bengal, where *Rostek et al.* [1993] have reported a local variation of $\Delta\delta = 0.3$‰, the largest difference expected between the modern and the LGM slopes (say, a=0.21 and a'=0.15 from section 5.2) leads to an underestimation of the salinity variation by only $\varepsilon = 0.6$, despite the low slope that amplifies this error. Such a bias lies within the error bar estimated when reconstructing paleosalinity.

6. Conclusion

We use atmospheric isotopic fluxes derived from a low-resolution GCM, which are consistent enough to reproduce the first-order $\delta^{18}O$ and salinity distribution and relationship in the northern Indian Ocean, particularly (1) a low slope (≈0.2-0.3) and a weak spatial correlation typical of the intertropical zone and (2) the contrast between the Arabian Sea and the Bay of Bengal mainly due to the runoff. Compared to the multibox model, the oceanic advection simulated by a GCM improves the relationship in the Bay of Bengal, especially by mixing the continental runoff.

Using atmospheric fluxes corresponding to LGM conditions provides some insight into the past $\delta^{18}O$ - salinity characteristics. The multibox model does not show any important change of the $\delta^{18}O$ - salinity relationship in either of the basins. Although the error in reconstructed paleosalinity is amplified by the low $\delta^{18}O$ - salinity slope, it does not appear stronger in this region than the typical uncertainty. A change in the oceanic advection is not accounted for in this perspective. This could only be achieved with a GCM simulation of glacial $\delta^{18}O$ and salinity fields.

Acknowledgments. The authors are grateful to O. Aumont and J. Orr at LSCE for the model use, to M.C. Bonin at the Centre Océanologique de Marseille for salinity analyses, to the reviewers for improving the manuscript, to R. Wardle for corrections, and to GEOMAR for their online map software using GMT. Simulations were run at CEA Grenoble on a CRAY 90. This work is supported by CNRS (PNEDC), the European Community (project ENV4-CT97-0659), and the IFCPAR (project 1809-1). All isotopic measurements considered in this study are available online at http://www.cerege.fr/donnees/general.htm.

References

Broecker, W. S., Salinity history of the northern Atlantic during the last deglaciation, *Paleoceanography*, *5*, 459-467, 1990.

Cadet, D., and G. Reverdin, Water vapor transport over the Indian Ocean during summer 1975, *Tellus*, 33, 476-487, 1981.

Craig, H., and L. I. Gordon, Deuterium and oxygen 18 variations in the ocean and the marine atmosphere, in *Stable Isotopes in Oceanographic Studies and Paleotemperatures*, edited by E. Tongiorgi, pp. 9-130, Lab. di Geol. Nucl., Cons. Naz. delle Ric., Pisa, Italy, 1965.

Dansgaard, W., Stable isotopes in precipitation, *Tellus*, *16*, 436-468, 1964.

Delaygue, G., J. Jouzel, and J.-C. Dutay, Salinity-oxygen 18 relationship simulated by an oceanic general circulation model, *Earth Planet. Sci. Lett.*, *178*, 113-123, 2000.

Duplessy, J.-C., Glacial to interglacial contrasts in the northern Indian Ocean, *Nature*, *295*, 494-498, 1982.

Duplessy, J.-C., A. W. H. Bé, and P. L. Blanc, Oxygen and carbon isotopic composition and biogeographic distribution of planktonic foraminifera in the Indian Ocean, *Paleogeogr. Paleoclimatol. Paleoecol.*, *33*, 9-46, 1981.

Duplessy, J.-C., L. Labeyrie, A. Juillet-Leclerc, F. Maitre, J. Duprat, and M. Sarnthein, Surface salinity reconstruction of the North Atlantic Ocean during the last glacial maximum, *Oceanol. Acta*, *14*, 311-324, 1991.

Fairbanks, R. G., The origin of continental shelf and slope water in the New York Bight and Gulf of Maine: Evidence from $H_2{}^{18}O/H_2{}^{16}O$ ratio measurements, *J. Geophys. Res.*, *87*, 5796-5808, 1982.

Ganssen, G., and D. Kroon, Evidence for Red Sea surface circulation from oxygen isotopes of modern surface waters and planktonic foraminiferal tests, *Paleoceanography*, *6*, 73-82, 1991.

Hansen, J., G. Russell, D. Rind, P. Stone, A. Lacis, S. Lebedeff, R. Ruedy, and L. Travis, Efficient three-dimensional global models for climate studies: Models I and II, *Mon. Weather Rev.*, *111*, 609-662, 1983.

Hastenrath, S., and L. Greischar, The monsoonal heat budget of the hydrosphere-atmosphere system in the Indian ocean sector, *J. Geophys. Res.*, *98*, 6869-6881, 1993.

Jouzel, J., G. L. Russell, R. J. Suozzo, R. D. Koster, J. W. C. White, and W. S. Broecker, Simulations of the HDO and $H_2{}^{18}O$ atmospheric cycles using the NASA GISS general circulation model: The seasonal cycle for present-day conditions, *J. Geophys. Res.*, *92*, 14739-14760, 1987.

Jouzel, J., R. D. Koster, R. J. Suozzo, and G. L. Russell, Stable water isotope behavior during the last glacial maximum: A general circulation model analysis, *J. Geophys. Res.*, *99*, 25791-25801, 1994.

Juillet-Leclerc, A., J. Jouzel, L. Labeyrie, and S. Joussaume, Modern and last glacial maximum sea surface $\delta^{18}O$ derived from an Atmospheric General Circulation Model, *Earth Planet. Sci. Lett.*, *146*, 591-605, 1997.

Levitus, S., R. Burgett, and T. P. Boyer, *World Ocean Atlas 1994, vol. 3: Salinity*, *NOAA Atlas, NESDIS*, 99 pp., U.S. Dept. of Commerce, Washington, D.C., 1994.

Madec, G., P. Delecluse, M. Imbard and C. Lévy, *OPA 8.1 Ocean General Circulation Model Reference Manual: Notes du Pôle de Modélisation* (on line), Institut Pierre-Simon-Laplace, Paris, 1998.

Miller, J. R., G. L. Russell, and G. Caliri, Continental-scale river flow in climate models, *J. Clim.*, *7*, 914-928, 1994.

Östlund, H. G., and G. Hut, Arctic Ocean water mass balance from isotope data, *J. Geophys. Res.*, *89*, 6373-6381, 1984.

Östlund, H., H. Craig, W. S. Broecker, and D. Spenser (Eds.), GEOSECS Atlantic, Pacific and Indian Ocean Expeditions, vol. 7, *Shorebased Data and Graphics*, Int. Decade of Ocean Explor., Natl. Science Found., Washington D. C., 1987.

Peixóto, J. P., and A. H. Oort, The atmospheric branch of the hydrological cycle and climate, in *Variations in the Global Water Budget*, edited by A. Street-Perrott, M. Beran, and R. Ratcliffe, pp. 5-65, D. Reidel, Norwell, Mass., 1983.

Perry, G. D., P. B. Duffy, and N. L. Miller, An extended data set of river discharges for validation of general circulation models, *J. Geophys. Res.*, *101*, 21339-21349, 1996.

Pierre, C., A. Vangriesheim, and E. Laube-Lenfant, Variability of water masses and of organic production-regeneration systems as related to eutrophic, mesotrophic and oligotrophic conditions in the northeast Atlantic Ocean, *J. Mar. Syst.*, *5*, 159-170, 1994.

Quadfasel, D., A. Frische, and A. Rubino, Hydrography, in *Cruise Report Sonne Cruise SO93*, edited by H. Kudra, *Rep. 112196*, pp. 9-19, Bundesanst. für Geowiss. und Rohstoffe, Hannover, Germany, 1994.

Ramesh, R., and M. M. Sarin, Stable isotope study of the Ganga (Ganges) River system, *J. Hydrol.*, *139*, 49-62, 1992.

Rohling, E. J., and G. R. Bigg, Paleosalinity and $\delta^{18}O$: A critical assessment, *J. Geophys. Res.*, *103*, 1307-1318, 1998.

Rostek, F., G. Ruhland, F. C. Bassinot, P. J. Muller, L. D. Labeyrie, Y. Lancelot, and E. Bard, Reconstructing sea surface temperature and salinity using $\delta^{18}O$ and alkenone records, *Nature*, *364*, 319-321, 1993.

Schäfer-Neth, C., Changes in the seawater salinity-oxygen isotope relation between last glacial and present: Sediment core data and OGCM modelling, *Paleoclimates*, *2*, 101-131, 1998.

Schmidt, G. A., Oxygen-18 variations in a global ocean model, *Geophys. Res. Lett.*, *25*, 1201-1204, 1998.

Schmidt, G. A., Error analysis of paleosalinity calculations, *Paleoceanography*, *14*, 422-429, 1999.

Schrag, D. P., G. Hampt, and D. W. Murray, Pore fluids constraints on the temperature and oxygen isotopic composition of the glacial ocean, *Science*, *272*, 1930-1932, 1996.

Trenberth, K. E., and C. J. Guillemot, Evaluation of the atmospheric moisture and hydrological cycle in the NCEP/NCAR reanalyses, *Clim. Dyn.*, *14*, 213-231, 1998.

E. Bard and C. Rollion, CEREGE (UMR 6635), Europôle Arbois BP 80, 13545 Aix-en-Provence, France.

G. Delaygue, Department of Geophysical Sciences, University of Chicago, 5734 S. Ellis Avenue, Chicago, IL 60637. (delaygue@geosci.uchicago.edu)

J.-C. Duplessy, J. Jouzel, and M. Stiévenard, LSCE (UMR 1572), Orme des Merisiers, CEA Saclay, 91191 Gif-sur-Yvette, France.

G. Ganssen, Department of Earth Sciences, Free University Amsterdam, De Boelelaan 1085, 1081 HV Amsterdam, Netherlands.

(Received September 3, 1999; revised September 21, 2000; accepted October 5, 2000.)